Polarization properties of optical phase conjugation by two-photon resonant degenerate four-wave mixing

Martti Kauranen, Daniel J. Gauthier, Michelle S. Malcuit, and Robert W. Boyd
The Institute of Optics, University of Rochester, Rochester, New York 14627
(Received 3 February 1989)

We develop a semiclassical theory of the polarization properties of phase conjugation by two-photon resonant degenerate four-wave mixing. The theory includes the effects of saturation by the pump waves. We solve the density-matrix equations of motion in steady state for a nonlinear medium consisting of stationary atoms with a ground and excited state connected by two-photon transitions. As an illustration of the general results, we consider an $S_0 \rightarrow S_0$ two-photon transition, which is known to lead to perfect polarization conjugation in the limit of third-order theory. We show that the fidelity of the polarization-conjugation process is degraded for excessively large pump intensities. The degradation can occur both due to transfer of population to the excited state and due to nonresonant Stark shifts. Theoretical results are compared to those of a recent experiment [Malcuit, Gauthier, and Boyd, Opt. Lett. **13**, 663 (1988)].

I. INTRODUCTION

Optical phase conjugation is a process that can remove in double pass the aberrations impressed on an optical wave in passing through a distorting medium. Ideally, the wave generated by the phase-conjugation process possesses two properties: (1) wave-front reversal: the scalar field amplitude of the generated wave is the complex conjugate of that of the incident wave and (2) polarization conjugation: the polarization vector of the generated field is the complex conjugate of that of the incident field. Polarization conjugation is often a desirable property because it can be used to correct for polarization distortions. Many interactions that can be used to produce a phase-conjugate wave front do not possess this second property. We will refer to a process that possesses both of the properties described above as a vector-phase-conjugation (VPC) process.

Polarization properties of phase conjugation have been studied theoretically by a number of researchers[1-10] within the context of third-order theory. In particular, Grynberg[1] and Ducloy and Bloch[2] have predicted that degenerate four-wave mixing (DFWM) based on two-photon atomic resonances will lead to VPC for arbitrary states of polarization of the two pump waves for an appropriate choice of atomic levels. This possibility has been tested experimentally by Malcuit *et al.*[11] using the $3S \rightarrow 6S$ two-photon transition of sodium. They observed high-fidelity VPC for pump intensities well below the two-photon saturation intensity, i.e., when the assumptions of Refs. 1 and 2 were satisfied. However, when the pump intensities were increased in order to increase the phase-conjugate reflectivity, the vector character of the phase-conjugation process was found to be severely degraded.

In order to explain these experimental results, we present in this paper a theory of DFWM resonantly enhanced by a two-photon-allowed atomic transition. Our theory treats the DFWM process for arbitrary states of polarization of the interacting fields, and includes the effects of saturation by the pump fields. Existing theories[12,13] of two-photon resonant phase conjugation that include saturation effects are restricted to the scalar case, i.e., to the case where all interacting fields have the same polarization.

II. THEORETICAL FORMULATION

We model the nonlinear optical medium as a collection of stationary atoms with a single ground state $|0\rangle$ connected by two-photon transitions through the intermediate states $|k'\rangle$ to a single excited state $|2\rangle$, as shown in Fig. 1. The atoms interact with an electromagnetic field of the form

$$\mathbf{E}(\mathbf{r},t)=\mathbf{E}_\omega(\mathbf{r},t)e^{-i\omega t}+\mathbf{E}_\omega^*(\mathbf{r},t)e^{i\omega t}\ , \tag{1}$$

where 2ω is close to the two-photon resonance frequency (i.e., $2\omega \approx \omega_{20}$, where $\hbar\omega_{20}$ is the energy difference between the excited and ground states), and where the fractional variation of $\mathbf{E}_\omega(\mathbf{r},t)$ in an optical period $2\pi/\omega$ is

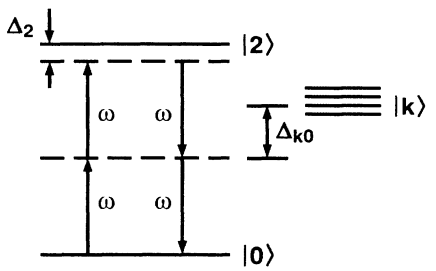

FIG. 1. Energy-level diagram showing the ground state $|0\rangle$ and the excited state $|2\rangle$ which are connected by two-photon transitions through the intermediate states $|k\rangle$.

small. Similarly, the atomic polarization of the medium, which acts as the source of the conjugate field, is represented as

$$\mathbf{P}(\mathbf{r},t)=\mathbf{P}_{\omega}(\mathbf{r},t)e^{-i\omega t}+\mathbf{P}^{*}_{\omega}(\mathbf{r},t)e^{i\omega t} . \tag{2}$$

We consider the case in which no intermediate state is resonantly excited. We therefore assume that the intermediate states do not acquire appreciable population and that there are no appreciable coherences among these states. Consequently, the only nonzero components of the density matrix are the ground-state population ρ_{00}, the excited-state population ρ_{22}, the one-photon coherences $\rho_{k'0}$ and $\rho_{2k'}$, and the two-photon coherence ρ_{20}. We assume that the excited-state population decays back to the ground state with a decay rate Γ. Hence population is conserved, i.e., $\rho_{00}+\rho_{22}=1$.

To simplify our working equations, we assume that for a subset $|k\rangle$ of intermediate states the detuning from the one-photon resonances is small compared to an optical frequency.[14] We hence introduce the slowly varying quantities σ_{ij} by means of the relations

$$\begin{aligned}&\rho_{00}=\sigma_{00},\quad \rho_{22}=\sigma_{22} ,\\ &\rho_{k0}=\sigma_{k0}e^{-i\omega t},\quad \rho_{2k}=\sigma_{2k}e^{-i\omega t} ,\\ &\rho_{20}=\sigma_{20}e^{-i2\omega t} ,\end{aligned} \tag{3}$$

and make the rotating-wave approximation to obtain the density-matrix equations of motion

$$\dot{w}=-\Gamma(w+1)+2\sum_{k}(i\alpha_{0k}\sigma_{k0}-i\alpha_{k0}\sigma_{0k}) , \tag{4}$$

$$\dot{\sigma}_{k0}=-(i\Delta_{k0}+\gamma_{k0})\sigma_{k0}+i\alpha_{k0}\frac{w-1}{2}-i\alpha_{k2}\sigma_{20} , \tag{5}$$

$$\dot{\sigma}_{2k}=-(i\Delta_{2k}+\gamma_{2k})\sigma_{2k}+i\alpha_{2k}\frac{w+1}{2}+i\alpha_{0k}\sigma_{20} , \tag{6}$$

$$\dot{\sigma}_{20}=-(i\Delta_{2}+\gamma_{20})\sigma_{20}+\sum_{k}(i\alpha_{k0}\sigma_{2k}-i\alpha_{2k}\sigma_{k0}) , \tag{7}$$

where $w=\sigma_{22}-\sigma_{00}$ is the population inversion, γ_{ij} is the decay constant for the σ_{ij} coherence, and the detunings are defined as $\Delta_2=\omega_{20}-2\omega$, $\Delta_{k0}=\omega_{k0}-\omega$, and $\Delta_{2k}=\omega_{2k}-\omega$. The one-photon coupling constants are defined as $\alpha_{k0}=\alpha^{*}_{0k}=-(\mathbf{d}_{k0}\cdot\mathbf{E}_{\omega})/\hbar$ and $\alpha_{2k}=\alpha^{*}_{k2}=-(\mathbf{d}_{2k}\cdot\mathbf{E}_{\omega})/\hbar$, where $\mathbf{d}_{ij}=-e\mathbf{r}_{ij}$ are the electric-dipole matrix elements.

We consider the case where the two-photon detuning Δ_2 is small and the one-photon detunings Δ_{k0} and Δ_{2k} are large compared to the decay rates of the corresponding coherences. In this case we can adiabatically eliminate[15] the one-photon coherences by formally setting $\dot{\sigma}_{k0}=0$ and $\dot{\sigma}_{2k}=0$ in Eqs. (5) and (6). These coherences are then given in terms of w and σ_{20} as

$$\begin{aligned}\sigma_{k0}&=\frac{\alpha_{k0}}{\Delta_{k0}}\frac{w-1}{2}-\frac{\alpha_{k2}}{\Delta_{k0}}\sigma_{20} ,\\ \sigma_{2k}&=-\frac{\alpha_{2k}}{\Delta_{k0}}\frac{w+1}{2}-\frac{\alpha_{0k}}{\Delta_{k0}}\sigma_{20} ,\end{aligned} \tag{8}$$

where we have taken $\Delta_{2k}=-\Delta_{k0}$. By substituting these expressions into Eqs. (4) and (7), we arrive at the two-photon, two-level density-matrix equations of motion[12,15–18]

$$\dot{w}=-\Gamma(w+1)-2i(Q_{02}\sigma_{20}-Q_{20}\sigma_{02}) , \tag{9}$$

$$\dot{\sigma}_{20}=-[i(\Delta_2+Q_{00}-Q_{22})+\gamma]\sigma_{20}-iQ_{20}w , \tag{10}$$

where $\gamma\equiv\gamma_{20}$, and the two-photon coupling constants are defined by

$$Q_{ij}=\sum_{k}\frac{\alpha_{ik}\alpha_{kj}}{\Delta_{k0}} . \tag{11}$$

The coupling constants Q_{00} and Q_{22} correspond to the Stark shifts of the ground and excited states, respectively, and Q_{20} corresponds to one-half of the two-photon Rabi frequency.[15]

We solve Eqs. (9) and (10) in steady state to find the inversion and the two-photon coherence:

$$w=-\frac{1+(\Delta_2+Q_{00}-Q_{22})^2/\gamma^2}{1+(\Delta_2+Q_{00}-Q_{22})^2/\gamma^2+4(1/\gamma\Gamma)|Q_{20}|^2} , \tag{12}$$

$$\sigma_{20}=i\frac{Q_{20}}{\gamma}\frac{1-i(\Delta_2+Q_{00}-Q_{22})/\gamma}{1+(\Delta_2+Q_{00}-Q_{22})^2/\gamma^2+4(1/\gamma\Gamma)|Q_{20}|^2} . \tag{13}$$

In the scalar limit, these solutions reduce to the ones obtained by Sargent *et al.*;[12] however, since our coupling constants α_{ij} depend on the state of polarization of the optical fields, we can treat the tensor nature of the interaction in our theory. Finally, the steady-state polarization amplitude $\mathbf{P}_{\omega}(\mathbf{r})=N\,\mathrm{Tr}(\mathbf{d}\sigma)$ for the medium is given by

$$\begin{aligned}\mathbf{P}_{\omega}(\mathbf{r})=&-N\sum_{k}\frac{\mathbf{d}_{0k}\alpha_{k0}}{\Delta_{k0}}-iN\sum_{k}\frac{\mathbf{d}_{0k}\alpha_{k2}+\mathbf{d}_{k2}\alpha_{0k}}{\Delta_{k0}}\frac{(Q_{20}/\gamma)[1-i(\Delta_2+Q_{00}-Q_{22})/\gamma]}{1+(\Delta_2+Q_{00}-Q_{22})^2/\gamma^2+4(1/\gamma\Gamma)|Q_{20}|^2}\\ &+N\sum_{k}\frac{\mathbf{d}_{0k}\alpha_{k0}-\mathbf{d}_{k2}\alpha_{2k}}{\Delta_{k0}}\frac{2(1/\gamma\Gamma)|Q_{20}|^2}{1+(\Delta_2+Q_{00}-Q_{22})^2/\gamma^2+4(1/\gamma\Gamma)|Q_{20}|^2} .\end{aligned} \tag{14}$$

III. PHASE CONJUGATION UTILIZING AN $S_0\rightarrow S_0$ TRANSITION

We now treat the case of phase conjugation by DFWM specialized to the geometry shown in Fig. 2. We assume that all interacting waves are infinite plane waves propagating almost parallel or antiparallel to the z axis. We consider the case of a $nS_0\rightarrow n''S_0$ two-photon transition because in the third-order limit this excitation scheme gives rise to perfect VPC.[1,2] This choice of levels also ap-

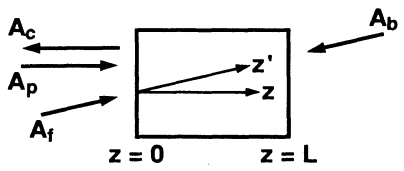

FIG. 2. Geometry for phase conjugation by DFWM with the strong pump waves A_f and A_b propagating along the $\pm z'$ directions, and the probe wave A_p and conjugate wave A_c propagating along the $\pm z$ directions. The angle between the two axes is assumed to be small, so that all fields are polarized in the x-y plane.

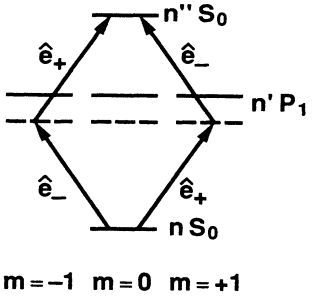

FIG. 3. Relevant states for the $nS_0 \rightarrow n''S_0$ two-photon excitation scheme. Circularly polarized field components can induce only the transitions shown.

proximates those of the experiment of Malcuit *et al.*[11] For this excitation scheme, the only intermediate states that connect the ground and excited states are the magnetic sublevels of the $n'P_1$ levels, as shown in Fig. 3. Note, for example, that an $\hat{\mathbf{e}}_\pm = \mp(\hat{\mathbf{x}} \pm i\hat{\mathbf{y}})/\sqrt{2}$ circularly polarized photon can interact[19] only with the $|nS_0, m=0\rangle \rightarrow |n'P_1, m=\pm 1\rangle$ transition or the $|n'P_1, m=\mp 1\rangle \rightarrow |n''S_0, m=0\rangle$ transition.

The diagrammatic analysis of Fig. 4 displays pictorially why third-order processes lead to perfect VPC for two-photon resonant media and why the fidelity of VPC can be degraded by higher-order processes. Note that in a perfect VPC process an $\hat{\mathbf{e}}_+$ circularly polarized probe photon leads to the generation of an $\hat{\mathbf{e}}_-$ circularly polarized conjugate photon, and vice versa. In Fig. 4(a), the pump intensity is assumed to be sufficiently low that only third-order processes can occur. The conjugate photon is then necessarily created by processes such as the one illustrated in which one photon from each pump field is absorbed and the probe and conjugate photons are necessarily emitted with equal and opposite angular momenta, producing perfect VPC. For high pump intensities, processes involving more than two pump photons can occur, and the vector nature of the VPC process can become degraded, since a photon can be emitted into the conjugate wave with the wrong circular polarization, as illustrated in Fig. 4(b).

To describe quantitatively the polarization properties of the two-photon resonant DFWM interaction, we must evaluate the two-photon coupling constants Q_{ij} and the sums over k in Eq. (14). To do this, we assume that the detunings for all relevant intermediate states are approximately equal and set $\Delta_{k0} = \Delta_1$ for all k. For all interacting waves propagating almost parallel or antiparallel to the z axis, the coupling constants and the sums over k can be expressed in terms of the two-photon matrix elements

$$M_{ij} = \sum_k r_{ik}^{(-)} r_{kj}^{(+)} = \sum_k r_{ik}^{(+)} r_{kj}^{(-)} ,$$

where $r_{ij}^{(\pm)} = \mp(x \pm iy)_{ij}/\sqrt{2}$. The coupling constants are found to be

$$\begin{aligned} Q_{00} &= -\frac{e^2}{\Delta_1 \hbar^2} M_{00} (\mathbf{E}_\omega \cdot \mathbf{E}_\omega^*) , \\ Q_{22} &= -\frac{e^2}{\Delta_1 \hbar^2} M_{22} (\mathbf{E}_\omega \cdot \mathbf{E}_\omega^*) , \\ Q_{20} &= -\frac{e^2}{\Delta_1 \hbar^2} M_{20} (\mathbf{E}_\omega \cdot \mathbf{E}_\omega) , \end{aligned} \tag{15}$$

and the sums over k in Eq. (14) are

$$\begin{aligned} &\sum_k \mathbf{d}_{0k} \alpha_{k0} = \frac{e^2}{\hbar} M_{00} \mathbf{E}_\omega , \quad \sum_k \mathbf{d}_{k2} \alpha_{2k} = \frac{e^2}{\hbar} M_{22} \mathbf{E}_\omega , \\ &\sum_k \mathbf{d}_{0k} \alpha_{k2} = \sum_k \mathbf{d}_{k2} \alpha_{0k} = \frac{e^2}{\hbar} M_{02} \mathbf{E}_\omega^* . \end{aligned} \tag{16}$$

The expression for the polarization amplitude $\mathbf{P}_\omega(\mathbf{r})$ is hence given by

$$\begin{aligned} \mathbf{P}_\omega(\mathbf{r}) = &-\frac{Ne^2}{\hbar \Delta_1} M_{00} \mathbf{E}_\omega + i \frac{N\hbar\Gamma}{2I_s^2} \frac{1 - i\gamma^{-1}(\Delta_2 + \omega_S |\mathbf{E}_\omega|^2/I_s)}{1 + \gamma^{-2}(\Delta_2 + \omega_S |\mathbf{E}_\omega|^2/I_s)^2 + |\mathbf{E}_\omega \cdot \mathbf{E}_\omega|^2/I_s^2} (\mathbf{E}_\omega \cdot \mathbf{E}_\omega) \mathbf{E}_\omega^* \\ &- \frac{N\hbar\omega_S}{2I_s^3} \frac{|\mathbf{E}_\omega \cdot \mathbf{E}_\omega|^2}{1 + \gamma^{-2}(\Delta_2 + \omega_S |\mathbf{E}_\omega|^2/I_s)^2 + |\mathbf{E}_\omega \cdot \mathbf{E}_\omega|^2/I_s^2} \mathbf{E}_\omega , \end{aligned} \tag{17}$$

where we have introduced the two-photon saturation intensity

$$I_s = \frac{|\Delta_1| \hbar^2 \sqrt{\gamma\Gamma}}{2e^2 |M_{20}|} , \tag{18}$$

and the Stark-shift parameter

$$\omega_S = -\frac{\Delta_1}{|\Delta_1|} \frac{\sqrt{\gamma\Gamma}(M_{00} - M_{22})}{2|M_{20}|} , \tag{19}$$

where $\omega_S|\mathbf{E}_\omega|^2/I_s$ gives the shift of the two-photon transition frequency.

The first term of Eq. (17) gives the linear contribution to the refractive index and arises from off-resonant, single-photon transitions originating from the ground state. The two remaining terms are the nonlinear part of the atomic polarization. Note that the second term has the vector character of $\mathbf{E}_\omega^*$ and the third term that of $\mathbf{E}_\omega$. By inspection of Eq. (17) we see that in the third-order limit the third term vanishes and the second gives rise to perfect VPC, in agreement with the predictions of Refs. 1 and 2.

For the DFWM geometry of Fig. 2, it is convenient to express the total field $\mathbf{E}_\omega(\mathbf{r})$ as

$$\mathbf{E}_\omega(\mathbf{r})=\mathbf{E}_0(\mathbf{r})+\mathbf{A}_p(z)e^{ikz}+\mathbf{A}_c(z)e^{-ikz}, \tag{20}$$

where $\mathbf{E}_0(\mathbf{r})=\mathbf{A}_f e^{ikz'}+\mathbf{A}_b e^{-ikz'}$ represents the field of the two counterpropagating pump waves, and $\mathbf{A}_p$ and $\mathbf{A}_c$ are the slowly varying probe and conjugate field amplitudes. We assume that the probe and conjugate fields are much weaker than the pump fields. We hence linearize the expression for the polarization with respect to the probe and conjugate field amplitudes about the amplitude $\mathbf{E}_0$ of the strong pump field, and obtain

$$\begin{aligned}\mathbf{P}_\omega(\mathbf{r})=&[\mathbf{P}_c(\mathbf{A}_c)+\mathbf{P}_c(\mathbf{A}_p^*)]e^{-ikz}\\&+[\mathbf{P}_p(\mathbf{A}_p)+\mathbf{P}_p(\mathbf{A}_c^*)]e^{ikz}.\end{aligned} \tag{21}$$

Here the amplitudes $\mathbf{P}_c(A_c)$ and $\mathbf{P}_c(\mathbf{A}_p^*)$ are contributions to the source term for the conjugate field that depend linearly on the conjugate field and the complex conjugate of the probe field, respectively. Analogously, $\mathbf{P}_p(\mathbf{A}_p)$ and $\mathbf{P}_p(\mathbf{A}_c^*)$ are the source terms for the probe field. Explicitly, we find that the second contribution of Eq. (21) (which represents coupling from the probe field into the conjugate field) is given by

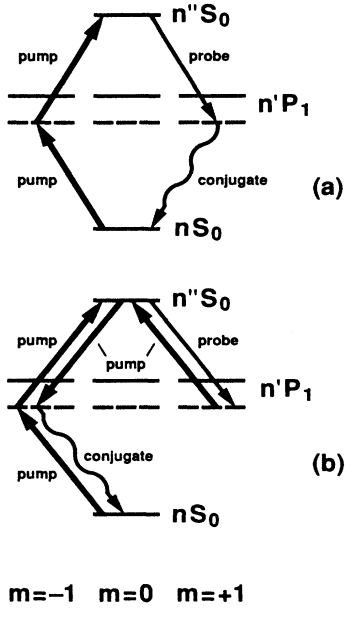

FIG. 4. Processes leading to phase conjugation in an $nS_0\rightarrow n''S_0$ two-photon excitation scheme. The thick arrows denote pump photons, the thin solid arrow the probe photon, and the thin wavy arrow the conjugate photon. (a) In a third-order process, the probe and conjugate photons are necessarily emitted in cascade, and perfect VPC is obtained. (b) In a fifth-order process the probe and conjugate photons need not be emitted in cascade, and in the example shown the conjugate photon is emitted with the wrong circular polarization.

$$\begin{aligned}\mathbf{P}_c(\mathbf{A}_p^*)=\frac{N\hbar\gamma}{I_s}\Bigg[&\frac{i}{2}\frac{(1-i\delta_2')\Gamma'}{1+(\delta_2')^2+|\mathbf{E}_0'\cdot\mathbf{E}_0'|^2}(\mathbf{E}_0'\cdot\mathbf{E}_0')\mathbf{A}_p^*+\frac{\delta_2'\omega_S'^2}{[1+(\delta_2')^2+|\mathbf{E}_0'\cdot\mathbf{E}_0'|^2]^2}|\mathbf{E}_0'\cdot\mathbf{E}_0'|^2(\mathbf{E}_0'\cdot\mathbf{A}_p^*)\mathbf{E}_0'\\&-\frac{[1+(\delta_2')^2]\omega_S'}{[1+(\delta_2')^2+|\mathbf{E}_0'\cdot\mathbf{E}_0'|^2]^2}(\mathbf{E}_0'\cdot\mathbf{E}_0')(\mathbf{E}_0'^*\cdot\mathbf{A}_p^*)\mathbf{E}_0'\\&-i\frac{(1-i\delta_2')\Gamma'\delta_2'\omega_S'}{[1+(\delta_2')^2][1+(\delta_2')^2+|\mathbf{E}_0'\cdot\mathbf{E}_0'|^2]}(\mathbf{E}_0'\cdot\mathbf{E}_0')(\mathbf{E}_0'\cdot\mathbf{A}_p^*)\mathbf{E}_0'^*\\&+\frac{1}{2}\frac{\Gamma'\omega_S'}{1+(\delta_2')^2+|\mathbf{E}_0'\cdot\mathbf{E}_0'|^2}(\mathbf{E}_0'\cdot\mathbf{E}_0')(\mathbf{E}_0'\cdot\mathbf{A}_p^*)\mathbf{E}_0'^*\\&+i\frac{(1-i\delta_2')\Gamma'\delta_2'\omega_S'}{[1+(\delta_2')^2][1+(\delta_2')^2+|\mathbf{E}_0'\cdot\mathbf{E}_0'|^2]^2}|\mathbf{E}_0'\cdot\mathbf{E}_0'|^2(\mathbf{E}_0'\cdot\mathbf{E}_0')(\mathbf{E}_0'\cdot\mathbf{A}_p^*)\mathbf{E}_0'^*\\&-i\frac{(1-i\delta_2')\Gamma'}{[1+(\delta_2')^2+|\mathbf{E}_0'\cdot\mathbf{E}_0'|^2]^2}(\mathbf{E}_0'\cdot\mathbf{E}_0')^2(\mathbf{E}_0'^*\cdot\mathbf{A}_p^*)\mathbf{E}_0'^*\Bigg],\end{aligned} \tag{22}$$

where we have introduced the dimensionless quantities $\mathbf{E}_0'=\mathbf{E}_0/\sqrt{I_s}$, $\Gamma'=\Gamma/\gamma$, $\omega_S'=\omega_S/\gamma$, and $\delta_2'=\delta_2/\gamma$, and the Stark-shifted detuning is defined as $\delta_2=\Delta_2+\omega_S|\mathbf{E}_0|^2/I_s$. By inspection of Eq. (22) it can be seen that only the first term has the correct tensor property for VPC, since it is the only term whose polarization will always be the complex conjugate of that of the probe wave. All other contributions lead to the generation of a conjugate field whose polarization can be different from the complex conjugate of that of the probe field.

Using the linearized expression for the nonlinear polarization [Eq. (21)] as a source term in the driven wave equation, we derive coupled amplitude equations governing the spatial evolution of the probe and conjugate fields in the constant-pump-amplitude limit.[20] These equations have the form

$$\frac{d\mathbf{A}_c}{dz}=-2\pi ik\langle \mathbf{P}_c(\mathbf{A}_c)+\mathbf{P}_c(\mathbf{A}_p^*)\rangle_\lambda ,$$
$$\frac{d\mathbf{A}_p^*}{dz}=-2\pi ik\langle \mathbf{P}_p^*(\mathbf{A}_c)+\mathbf{P}_p^*(\mathbf{A}_p^*)\rangle_\lambda , \tag{23}$$

where $k=n\omega/c$, and where the angular brackets denote a spatial average over a period of the fringe pattern created by the interference of the two pump waves. Spatial averaging is necessary in order to extract the phase-matched part of the polarization driving the probe and conjugate fields [Eq. (21)]. Equations (23) constitute a set of coupled linear differential equations, and hence they can be solved directly; however, the form of the solution is extremely complicated. Instead, we obtain a solution for the case of a medium sufficiently thin that the probe amplitude can be assumed to remain constant and that the effects of absorption on the generated conjugate field can be ignored. Then Eqs. (23) reduce to the single equation

$$\frac{d\mathbf{A}_c}{dz}=-2\pi ik\langle \mathbf{P}_c(\mathbf{A}_p^*)\rangle_\lambda . \tag{24}$$

To characterize the polarization properties of the generated conjugate field, we calculate the fraction of the conjugate field having a polarization vector that is the complex conjugate of that of the original probe field. To do this, we introduce the polarization unit vector of the probe field $\hat{\epsilon}_p$ such that $\mathbf{A}_p=A_p\hat{\epsilon}_p$, and we decompose the conjugate field in the form $\mathbf{A}_c=A_G\hat{\epsilon}_G+A_B\hat{\epsilon}_B$, where $\hat{\epsilon}_G\equiv\hat{\epsilon}_p^*$ is the polarization conjugate of the probe field (the "good" component, i.e., the polarization-conjugate component) and $\hat{\epsilon}_B$ (the "bad" component) is the polarization unit vector orthogonal to $\hat{\epsilon}_G$, i.e., $\hat{\epsilon}_B\cdot\hat{\epsilon}_G^*=0$. When decomposed into the good and bad polarization components, Eq. (24) becomes

$$\frac{dA_G}{dz}=i\kappa_G A_p^*,\quad \frac{dA_B}{dz}=i\kappa_B A_p^* , \tag{25}$$

where we have introduced the coupling constants κ_G and κ_B for the generation of the polarization components $\hat{\epsilon}_G$ and $\hat{\epsilon}_B$, respectively. The coupling constants are related to the polarization amplitude $\mathbf{P}_c(\mathbf{A}_p^*)$ by the equations

$$\kappa_G=-\frac{2\pi k\langle \mathbf{P}_c(\mathbf{A}_p^*)\rangle_\lambda\cdot\hat{\epsilon}_G^*}{A_p^*},$$
$$\kappa_B=-\frac{2\pi k\langle \mathbf{P}_c(\mathbf{A}_p^*)\rangle_\lambda\cdot\hat{\epsilon}_B^*}{A_p^*} . \tag{26}$$

The phase-conjugate reflectivities associated with the generation of the $\hat{\epsilon}_G$ and $\hat{\epsilon}_B$ polarization components can be obtained from the solutions of Eqs. (25) with the boundary condition $\mathbf{A}_c(L)=0$, and are given by

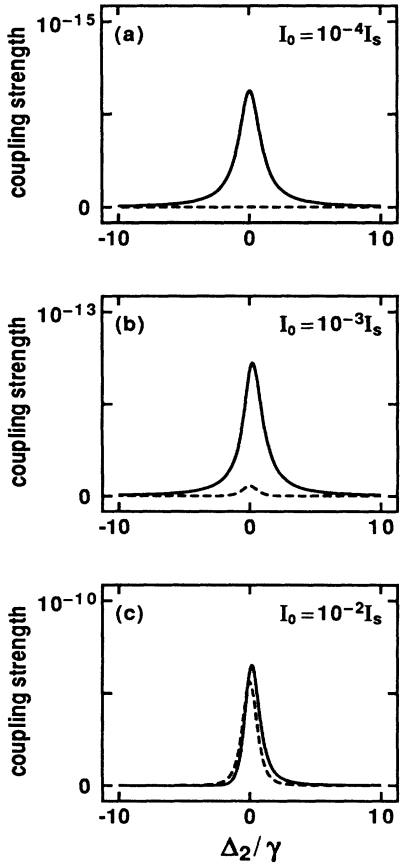

FIG. 5. Coupling strengths [in units of $(2\pi kN\hbar\gamma/I_s)^2$] for the good polarization component $\hat{\epsilon}_G\equiv\hat{\epsilon}_p^*$ (solid line) and the orthogonal (bad) polarization component $\hat{\epsilon}_B$ (dashed line) of the conjugate wave as functions of the detuning Δ_2 from the two-photon resonance for several different values of the summed pump intensity $I_0=I_f+I_b$ with $I_f=I_b$. (a) For a very low pump intensity ($I_0=10^{-4}I_s$), perfect VPC behavior is obtained. (b) For $I_0=10^{-3}I_s$, a slight degradation of the VPC process is already evident. (c) For $I_0=10^{-2}I_s$, the VPC process is almost totally degraded even though the pump intensity is still much lower than the two-photon saturation intensity. In all cases, the pump waves have linear and parallel polarizations. The material parameters are $\Gamma/\gamma=5\times10^{-4}$ and $\omega_S/\gamma=-0.1$, and the probe polarization is described by Eq. (31) with $\theta=45°$ and φ arbitrary.

$$R_G=|A_G(0)|^2/|A_p(0)|^2=|\kappa_G|^2L^2$$

and

$$R_B=|A_B(0)|^2/|A_p(0)|^2=|\kappa_B|^2L^2\ ,$$

where L is the length of the nonlinear medium. The quantities $|\kappa_G|^2$ and $|\kappa_B|^2$ are hence the coupling strengths for the generation of the polarization-conjugate component $\hat{\epsilon}_G$ and the orthogonal component $\hat{\epsilon}_B$, respectively.

As noted earlier, only the first term in Eq. (22) necessarily leads to VPC, i.e., has only an $\hat{\epsilon}_G$ component. We decompose the other terms, whose polarizations are determined by factors such as $(\mathbf{E}_0\cdot\mathbf{A}_p^*)\mathbf{E}_0$, into the basis of $\hat{\epsilon}_G$ and $\hat{\epsilon}_B$ as follows:

$$\begin{aligned}
(\mathbf{E}_0\cdot\mathbf{A}_p^*)\mathbf{E}_0&=|\mathbf{E}_0|^2A_p^*(G_1\hat{\epsilon}_G+B_1\hat{\epsilon}_B)\ ,\\
(\mathbf{E}_0^*\cdot\mathbf{A}_p^*)\mathbf{E}_0&=|\mathbf{E}_0|^2A_p^*(G_2\hat{\epsilon}_G+B_2\hat{\epsilon}_B)\ ,\\
(\mathbf{E}_0\cdot\mathbf{A}_p^*)\mathbf{E}_0^*&=|\mathbf{E}_0|^2A_p^*(G_3\hat{\epsilon}_G+B_3\hat{\epsilon}_B)\ ,\\
(\mathbf{E}_0^*\cdot\mathbf{A}_p^*)\mathbf{E}_0^*&=|\mathbf{E}_0|^2A_p^*(G_4\hat{\epsilon}_G+B_4\hat{\epsilon}_B)\ ,
\end{aligned}\tag{27}$$

where the coefficients G_i and B_i depend only on the polarizations and phases of the interacting fields. By using Eqs. (22), (26), and (27), we find that the coupling constant κ_G giving rise to the polarization-conjugate component is given by

$$\begin{aligned}
\kappa_G=-\frac{2\pi kN\hbar\gamma}{I_s}\Bigg\langle&\frac{i}{2}\frac{(1-i\delta_2')\Gamma'}{1+(\delta_2')^2+|\mathbf{E}_0'\cdot\mathbf{E}_0'|^2}(\mathbf{E}_0'\cdot\mathbf{E}_0')+\frac{\delta_2'\omega_S'^2}{[1+(\delta_2')^2+|\mathbf{E}_0'\cdot\mathbf{E}_0'|^2]^2}|\mathbf{E}_0'\cdot\mathbf{E}_0'|^2|\mathbf{E}_0'|^2G_1\\
&-\frac{[1+(\delta_2')^2]\omega_S'}{[1+(\delta_2')^2+|\mathbf{E}_0'\cdot\mathbf{E}_0'|^2]^2}(\mathbf{E}_0'\cdot\mathbf{E}_0')|\mathbf{E}_0'|^2G_2-i\frac{(1-i\delta_2')\Gamma'\delta_2'\omega_S'}{[1+(\delta_2')^2][1+(\delta_2')^2+|\mathbf{E}_0'\cdot\mathbf{E}_0'|^2]}(\mathbf{E}_0'\cdot\mathbf{E}_0')|\mathbf{E}_0'|^2G_3\\
&+\frac{1}{2}\frac{\Gamma'\omega_S'}{1+(\delta_2')^2+|\mathbf{E}_0'\cdot\mathbf{E}_0'|^2}(\mathbf{E}_0'\cdot\mathbf{E}_0')|\mathbf{E}_0'|^2G_3\\
&+i\frac{(1-i\delta_2')\Gamma'\delta_2'\omega_S'}{[1+(\delta_2')^2][1+(\delta_2')^2+|\mathbf{E}_0'\cdot\mathbf{E}_0'|^2]^2}|\mathbf{E}_0'\cdot\mathbf{E}_0'|^2(\mathbf{E}_0'\cdot\mathbf{E}_0')|\mathbf{E}_0'|^2G_3\\
&-i\frac{(1-i\delta_2')\Gamma'}{[1+(\delta_2')^2+|\mathbf{E}_0'\cdot\mathbf{E}_0'|^2]^2}(\mathbf{E}_0'\cdot\mathbf{E}_0')^2|\mathbf{E}_0'|^2G_4\Bigg\rangle_\lambda\ ,
\end{aligned}\tag{28}$$

where we have written the results in terms of the dimensionless quantities introduced in Eq. (22). The expression for the coupling constant κ_B is given by an expression of the same form as Eq. (28) with the first term omitted and with G_i replaced by B_i in each remaining term.

There are two mechanisms that can degrade the VPC process. One of them is the transfer of population from the ground state to the excited state. This mechanism becomes significant for pump intensities of the order of the two-photon saturation intensity, i.e., $|\mathbf{E}_0|^2\sim I_s$. The other mechanism that can degrade the VPC process is the Stark shift of the two-photon resonance frequency. This effect becomes important when $\omega_S|\mathbf{E}_0|^2/I_s\sim\Gamma$, i.e., when the Stark shift of the two-photon transition frequency is of the order of the population decay rate of the transition. For large values of the Stark-shift parameter, this effect may become significant at pump intensities well below the saturation intensity. Therefore the relative importance of the two mechanisms depends on the ratio of Γ to ω_S.

IV. RESULTS FOR SPECIFIC PUMP-WAVE POLARIZATIONS

In this section, we treat four special cases of pump-wave polarizations and determine the coupling constants κ_G and κ_B for the generation of the two polarization components of the conjugate wave. An efficient VPC process has a high coupling strength $|\kappa_G|^2$ for the good polarization component $\hat{\epsilon}_G$, and zero coupling strength $|\kappa_B|^2$ for the bad component $\hat{\epsilon}_B$. A measure of the fidelity of the polarization conjugation process is the quantity

$$F_{\mathrm{VPC}}=\frac{|\kappa_G|^2}{|\kappa_G|^2+|\kappa_B|^2}\ ,\tag{29}$$

which gives the fraction of the total conjugate field having the proper state of polarization. In the results presented below, the quantity F_{VPC} is evaluated at the detuning Δ_2 from the two-photon resonance which produces the largest value of $|\kappa_G|^2$. In all cases, we give the coupling strengths in units of $(2\pi kN\hbar\gamma/I_s)^2$.

The first case we consider is that of pump waves with linear and parallel polarizations. The total pump field $\mathbf{E}_0$ can then be represented as

$$\mathbf{E}_0=(A_fe^{ikz'}+A_be^{-ikz'})\hat{\mathbf{x}}\ .\tag{30}$$

For future convenience we define $I_i=|A_i|^2$. For a probe wave in an arbitrary state of polarization, we represent its polarization unit vector as

$$\hat{\epsilon}_p=\cos\theta\,\hat{\mathbf{x}}+\sin\theta e^{i\varphi}\hat{\mathbf{y}}\ ,\tag{31}$$

and hence our basis vectors are given by $\hat{\epsilon}_G\equiv\hat{\epsilon}_p^*=\cos\theta\,\hat{\mathbf{x}}+\sin\theta e^{-i\varphi}\hat{\mathbf{y}}$ and by $\hat{\epsilon}_B=-\sin\theta\,\hat{\mathbf{x}}$

$+\cos\theta e^{-i\varphi}\hat{\mathbf{y}}$. Using Eqs. (30) and (31), we find that the factors G_i and B_i defined by Eqs. (27) are given by

$$G_1 = G_4^* = \cos^2\theta \frac{\mathbf{E}_0 \cdot \mathbf{E}_0}{|\mathbf{E}_0|^2}, \quad G_2 = G_3 = \cos^2\theta ,$$

$$B_1 = B_4^* = -\cos\theta \sin\theta \frac{\mathbf{E}_0 \cdot \mathbf{E}_0}{|\mathbf{E}_0|^2} , \tag{32}$$

$$B_2 = B_3 = -\cos\theta \sin\theta .$$

Since these expressions do not contain the phase angle φ, the VPC fidelity depends on the polarization state of the probe wave only through the parameter θ.

In Fig. 5 we have plotted the coupling strengths $|\kappa_G|^2$ and $|\kappa_B|^2$ as functions of the detuning Δ_2 from the two-photon resonance for different values of the sum of the pump-wave intensities $I_0 = I_f + I_b$ for the case $I_f = I_b$. We take the probe polarization to be described by $\theta = 45°$ (with φ arbitrary). The polarization ellipse of such a wave has an axis inclined at 45° to the x direction. The normalized population decay constant is taken to be $\Gamma/\gamma = 5 \times 10^{-4}$ and the normalized Stark-shift parameter is taken to be $\omega_S/\gamma = -0.1$. These values correspond to the parameters for the $3S \rightarrow 6S$ two-photon resonance of sodium,[21,22] for which $\Gamma = 3.3 \times 10^6$ s^{-1}. Figure 5(a) shows that at very low pump intensities the interaction leads to perfect VPC, i.e., $|\kappa_G|^2 \gg |\kappa_B|^2$. The VPC character of the process becomes degraded, however, as the pump intensity is increased, as shown in Figs. 5(b) and 5(c). In fact, for these particular values of the material parameters, the VPC character of the interaction is lost almost completely for pump intensities as small as 1% of the saturation intensity. For the present case where $\omega_S/\Gamma = 200$, the Stark shift of the two-photon transition frequency is the dominant mechanism leading to the degradation of the VPC process. Polarization rotation experiments in a two-photon resonant medium are also known to be affected by the presence of nonresonant Stark shifts.[23,24]

In Fig. 6 we have plotted the coupling strengths for the case in which the Stark-shift parameter ω_S vanishes but in which all the other material parameters are the same as in Fig. 5. High-fidelity VPC is now obtained using much higher pump intensities than in the case of Fig. 5, and consequently VPC with much larger reflectivities can be obtained in the present case. We see that the two polarization components of the conjugate field become comparable in magnitude when the sum of the pump-wave intensities is of the order of the saturation intensity. For this case the transfer of population to the excited state is the mechanism leading to the degradation of the VPC process. However, for pump intensities comparable to the saturation intensity, it is possible to obtain good VPC fidelity by tuning the laser frequency away from the exact two-photon resonance.

In Fig. 7 we see how the coupling strengths depend on the polarization of the probe wave. We show the results only as functions of θ since the predictions do not depend on the phase angle φ [see Eq. (31)]. The material parameters are taken to be the same as in Fig. 5 and the sum of the pump-wave intensities is taken to be

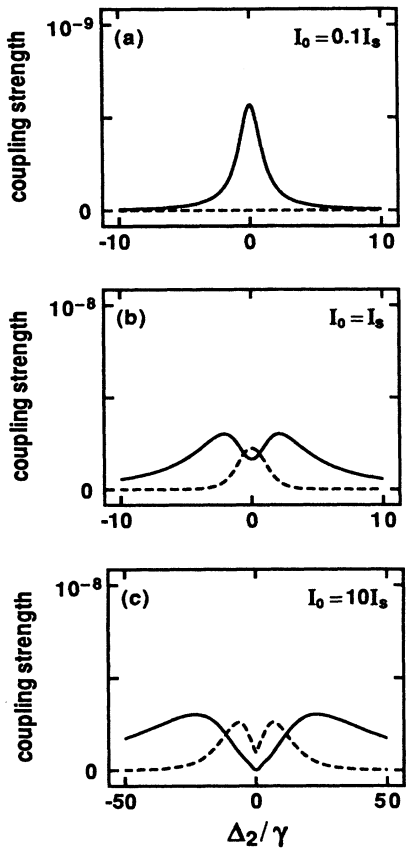

FIG. 6. Coupling strengths for the good (solid line) and bad (dashed line) polarization components of the conjugate wave for the case in which the Stark-shift parameter vanishes ($\omega_S = 0$) but in which the other material and experimental parameters are the same as in Fig. 5. (a) $I_0 = 0.1I_s$, (b) $I_0 = I_s$, (c) $I_0 = 10I_s$. We see that good VPC with a higher coupling strength than in Fig. 5 can now be obtained.

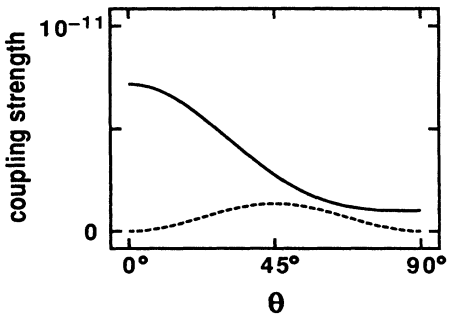

FIG. 7. Coupling strengths for the good (solid line) and bad (dashed line) polarization components as functions of the angle θ and for any value of φ. The state of polarization of the probe wave is determined by the parameter θ and the phase angle φ [see Eq. (31)] but the results are independent of φ. The pump waves have linear and parallel polarizations, and equal intensities with $I_0 = I_f + I_b = 4 \times 10^{-3} I_s$. The material parameters are the same as in Fig. 5. For the case of low pump intensities where the VPC process is ideal, the coupling strength for the good component is constant for all values of θ and the coupling strength for the bad component vanishes.

$I_0 = I_f + I_b = 4\times 10^{-3} I_s$ with $I_f = I_b$. When the probe field is linearly polarized along the pump polarization direction ($\theta = 0°$), the conjugate wave is seen to be the polarization conjugate of the probe wave. This result is obtained because in this case the interaction is effectively scalar. As θ is increased, the VPC fidelity is seen to degrade rapidly. However, when the probe polarization is linear and orthogonal to the pump polarization ($\theta = 90°$), perfect VPC is again obtained. Perfect VPC occurs for this choice of polarizations because B_i (and G_i) vanishes for all i [see Eqs. (27)], and hence κ_B vanishes identically. Since the probe wave polarization is orthogonal to that of the pump waves, no grating associated with the interference of the probe and pump waves is formed (i.e., $B_i = G_i = 0$). The only contribution to the phase-conjugate signal is hence the contribution due to the two-photon coherence induced by the two pump waves, and this contribution always leads to perfect VPC.

We have also analyzed the case of linear and orthogonal pump-wave polarizations. We find that this geometry never leads to high-fidelity VPC because $|\kappa_B|$ is comparable to $|\kappa_G|$. In this case, the polarization state of the conjugate field depends in a complicated way on that of the probe field.

We next treat the cases of circular pump-wave polarizations. For the case of co-rotating pump-wave polarizations, there is no two-photon coupling between the $|nS_0\rangle$ and $|n''S_0\rangle$ states, and hence no phase-conjugate field is generated. The case of circular and counter-rotating pump-wave polarizations does lead to the generation of a phase-conjugate field and has been shown to produce perfect VPC in the third-order limit for any isotropic material.[4-7] To treat this case, we express the total pump field as

$$\mathbf{E}_0 = A_f e^{ikz'}\hat{\mathbf{e}}_+ + A_b e^{-ikz'}\hat{\mathbf{e}}_- , \tag{33}$$

where as before $\hat{\mathbf{e}}_\pm = \mp(\hat{\mathbf{x}} \pm i\hat{\mathbf{y}})/\sqrt{2}$. We now find it convenient to represent the probe polarization vector as

$$\hat{\boldsymbol{\epsilon}}_p = -\cos\beta\,\hat{\mathbf{e}}_- - \sin\beta e^{i\eta}\hat{\mathbf{e}}_+ , \tag{34}$$

so that $\hat{\boldsymbol{\epsilon}}_G \equiv \hat{\boldsymbol{\epsilon}}_p^* = \cos\beta\,\hat{\mathbf{e}}_+ + \sin\beta e^{-i\eta}\hat{\mathbf{e}}_-$ and $\hat{\boldsymbol{\epsilon}}_B = -\sin\beta\,\hat{\mathbf{e}}_+ + \cos\beta e^{-i\eta}\hat{\mathbf{e}}_-$. The coefficients G_i and B_i then become

$$G_1 = G_4^* = -\frac{A_f A_b}{I_f + I_b}, \quad G_2 = \frac{I_f\cos^2\beta + I_b\sin^2\beta}{I_f + I_b} ,$$

$$G_3 = \frac{I_f\sin^2\beta + I_b\cos^2\beta}{I_f + I_b}, \quad B_1 = B_4 = 0 , \tag{35}$$

$$B_2 = -B_3 = \frac{(I_b - I_f)\cos\beta\sin\beta}{I_f + I_b} .$$

Note that these results do not depend on the phase angle η of the polarization vector of the probe wave. Comparison of Eqs. (35) with Eqs. (32) reveals some qualitative differences between the present case and that of linear and parallel pump-wave polarizations. Since B_1 and B_4 vanish but G_1 and G_4 do not, there are now additional terms in Eq. (22) that contribute only to κ_G and not to κ_B. The coefficient κ_B is now proportional to ω_S and perfect VPC is obtained whenever the Stark-shift parameter vanishes, for any pump intensity. In addition, when the intensities of the two pump waves are equal, the coefficients B_2 and B_3 also vanish, and hence for the case of balanced pumping perfect VPC is obtained even when the Stark-shift parameter does not vanish.

In Fig. 8 we have plotted the line shapes of the coupling strengths for different pump intensity ratios I_f/I_b keeping the sum of the pump intensities fixed such that $I_f + I_b = 2I_s$. The values of the material parameters are taken to be the same as in Fig. 5. The probe wave is taken to have an arbitrary linear polarization, corresponding

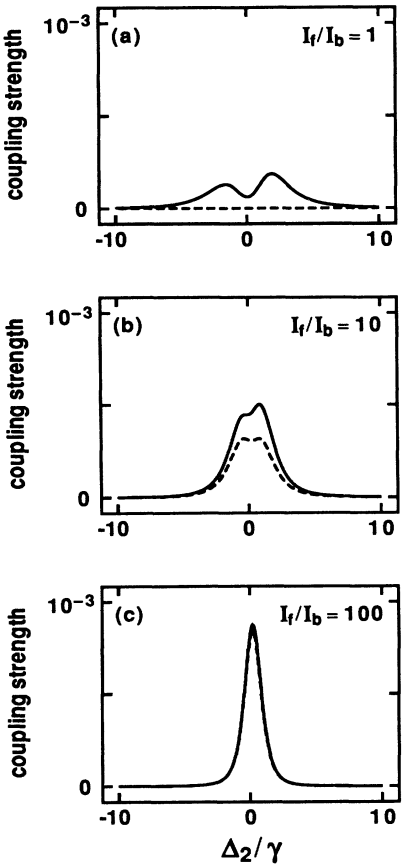

FIG. 8. Coupling strengths for the good (solid line) and bad (dashed line) polarization components of the conjugate wave as functions of the two-photon detuning Δ_2 for various ratios of the forward and backward pump intensities. The pump-wave polarizations are circular and counter-rotating and the sum of the pump intensities is kept fixed at $I_0 = 2I_s$. The material parameters are the same as in Fig. 5, and the probe polarization is described by Eq. (34) with $\beta = 45°$ and η arbitrary. (a) For equal pump intensities ($I_f/I_b = 1$) perfect VPC is obtained even though the line shape shows strong saturation. (b) $I_f/I_b = 10$. (c) For $I_f/I_b = 100$, the VPC process is almost totally degraded even though the line shape is not noticeably broadened.

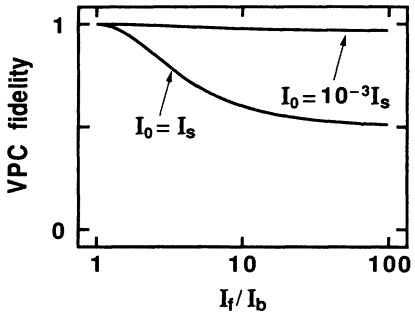

FIG. 9. Fidelity of the VPC process as defined by Eq. (29) plotted as a function of the ratio of the pump intensities. The pump-wave polarizations are circular and counter-rotating. The material parameters are the same as in Fig. 5. For low pump intensities ($I_0 = 10^{-3} I_s$), the VPC process is almost perfect (since the fidelity is near 1) for any value of the intensity ratio. For higher pump intensities ($I_0 = I_s$) the VPC behavior is degraded by the use of imbalanced pumping.

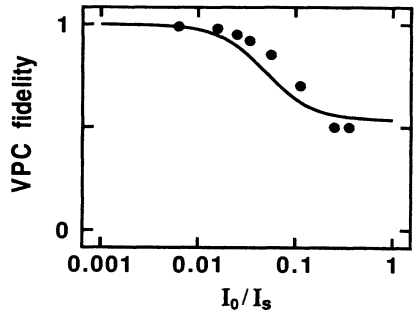

FIG. 10. Fidelity of the VPC process as a function of the sum of the pump intensities for linear and parallel pump-wave polarizations. The material parameters are the same as in Fig. 5, except that we have taken $\Gamma = 10^9\ s^{-1}$ implying that the normalized Stark-shift parameter is $\omega_S/\gamma = -1.8$, and the normalized population decay constant is $\Gamma/\gamma = 0.15$ corresponding to a saturation intensity of $I_s \approx 32\ MW\,cm^{-2}$. The dots are the experimental data from Ref. 11.

to $\beta = 45°$ with η arbitrary in Eq. (34). Figure 8(a) shows that perfect VPC occurs for equal pump-wave intensities, even though the line shape shows that the process is strongly saturated. As the pump imbalance is increased [Figs. 8(b) and 8(c)], the VPC character of the process is degraded but the line shapes show less broadening. The lack of broadening is due to the fact that the saturation of the two-photon transition for this choice of pump-wave polarizations depends on the pump-wave intensities only through the product $I_f I_b$.

In Fig. 9 we have plotted the VPC fidelity as defined in Eq. (29) as a function of the pump intensity ratio for two different values of the sum of the forward and backward pump intensities. The material parameters are again the same as in Fig. 5. For weak pump waves ($I_0 = I_f + I_b = 10^{-3} I_s$), nearly perfect VPC is obtained for any intensity ratio. For $I_0 = I_s$, the VPC fidelity is perfect when the pump intensities are equal but is almost totally degraded for pump intensity ratios greater than 10. These results are quite encouraging from a practical point of view because they show that the pump-wave intensities need to be balanced only to within a factor of 2 for high-fidelity VPC to occur.

V. COMPARISON TO EXPERIMENT

We now compare our theoretical results with those of the experiment of Malcuit *et al.*[11] The experiment studied the case of linear and parallel pump-wave polarizations, and utilized the $3S \rightarrow 6S$ two-photon transition of sodium. A pulsed dye laser with a pulse duration of ~ 15 ns was used. In the experiment it was found that the VPC fidelity was severely degraded when the sum of the pump-wave intensities was of the order of the saturation intensity, estimated to be $I_s = 2\ MW\,cm^{-2}$. Figure 5, which was plotted using the material parameters for the $3S \rightarrow 6S$ two-photon transition of sodium, predicts degradation of VPC at a pump intensity which is much smaller than the saturation intensity. Since the laser pulse length was much shorter than the population decay time $1/\Gamma \approx 300$ ns, steady-state conditions were never reached in the experiment. Due to the transient nature of the excitation and due to the depletion of the excited-state population by amplified spontaneous emission, we believe that the effective population decay time of the interaction is much shorter than 300 ns. In order to obtain a good fit to the experimental data, we have assumed an effective population decay time of $1/\Gamma = 1$ ns. In this case, the material parameters become $I_s = 32\ MW\,cm^{-2}$, $\omega_S/\gamma = -1.8$, and $\Gamma/\gamma = 0.15$. In Fig. 10 we have plotted the VPC fidelity [Eq. (29)] as a function of the sum of the pump intensities for these values of material parameters. The experimental data are shown for comparison.

VI. CONCLUSIONS

We have developed a theory that describes the polarization properties of phase conjugation by two-photon resonant DFWM. The theory includes the effects of saturation by the pump waves. We have treated in detail the case of $S_0 \rightarrow S_0$ two-photon excitation. Our results show that two mechanisms can lead to the degradation of the VPC process: the transfer of population to the excited state and the Stark shift of the two-photon resonance frequency.

The primary conclusions of the paper are as follows: the use of circular and counter-rotating pump-wave polarizations is the best configuration for producing high-fidelity VPC with high reflectivity. In this case perfect VPC is obtained for arbitrary high pump intensities as long as the intensities are equal. For the case of linear and parallel pump-wave polarizations, VPC with high reflectivity can be obtained for transitions where the Stark-shift parameter is small.

ACKNOWLEDGMENTS

We gratefully acknowledge discussions of this work with A. Jacobs and with G. Grynberg. This work was supported by U.S. Office of Naval Research Grant No. N00014-86-K-0746. A NATO travel grant is gratefully acknowledged. D.J.G. received additional support from U.S. Army Research Office University Research Initiative.

[1]G. Grynberg, Opt. Commun. **48**, 432 (1984).
[2]M. Ducloy and D. Bloch, Phys. Rev. A **30**, 3107 (1984).
[3]M. Ducloy, R. K. Raj, and D. Bloch, Opt. Lett. **7**, 60 (1982).
[4]S. Saikan and M. Kiguchi, Opt. Lett. **7**, 555 (1982).
[5]S. Saikan, J. Opt. Soc. Am. **72**, 514 (1982).
[6]G. Martin, L. L. Lam, and R. W. Hellwarth, Opt. Lett. **5**, 185 (1980).
[7]V. N. Blaschuk, B. Ya. Zel'dovich, A. V. Mamaev, N. F. Pilipetsky, and V. V. Shkunov, Kvant. Elektron. (Moscow) **7**, 627 (1980) [Sov. J. Quantum Electron. **10**, 356 (1980)].
[8]T. Wilson, D. K. Saldin, and L. Solymar, Opt. Commun. **39**, 11 (1981).
[9]T. Wilson, D. K. Saldin, and L. Solymar, Opt. Acta **29**, 1041 (1982).
[10]P. Yeh, Opt. Commun. **51**, 195 (1984).
[11]M. S. Malcuit, D. J. Gauthier, and R. W. Boyd, Opt. Lett. **13**, 663 (1988).
[12]M. Sargent III, S. Ovadia, and M. H. Lu, Phys. Rev. A **32**, 1596 (1985).
[13]T. Fu and M. Sargent III, Opt. Lett. **5**, 433 (1980).
[14]This could be relaxed as is done, for example, in Ref. 12. In this case, the definitions of the two-photon coupling constants in Eqs. (11) would be somewhat modified. However, for most feasible two-photon excitation schemes, it is sufficient to consider only the intermediate states close to the one-photon resonance.
[15]L. Allen and C. R. Stroud, Jr., Phys. Rep. **91**, 1 (1982).
[16]M. Takatsuji, Phys. Rev. A **11**, 619 (1975).
[17]D. Grischkowsky, M. M. T. Loy, and P. F. Liao, Phys. Rev. A **12**, 2514 (1975).
[18]G. Grynberg, M. Devaud, and C. Flytzanis, J. Phys. (Paris) **41**, 931 (1980).
[19]R. D. Cowan, *The Theory of Atomic Structure and Spectra* (University of California Press, Berkeley, 1981).
[20]By constant pump-wave amplitudes we mean that their complex vector amplitudes remain unchanged in the process.
[21]F. Biraben, B. Cagnac, E. Giacobino, and G. Grynberg, J. Phys. B **10**, 2369 (1977).
[22]R. B. Miles and S. E. Harris, IEEE J. Quantum Electron. **QE-9**, 470 (1973).
[23]P. F. Liao and G. C. Bjorklund, Phys. Rev. Lett. **36**, 584 (1976).
[24]P. F. Liao and G. C. Bjorklund, Phys. Rev. A **15**, 2009 (1977).